# Investigation of refractive index and group velocity of metal coated dielectric spherical nanocomposites within both passive and active dielectric cores

**Sh Getachew**
Wolkite University, Department of Physics, P. O. Box 07, Wolkite, Ethiopia

Email: shewa.getachew@wku.edu.et

**Abstract**
This research paper focuses on studying how light behaves in metal-coated dielectric spherical Nano composites. It investigates different types of light propagation, such as slow, backward, and fast lights. The paper examines the theoretical aspects of these phenomena in composite materials, specifically when spherical Nano inclusions are embedded in either active or passive dielectric cores, or when dielectric-coated metal spherical Nano inclusions are embedded in active or passive dielectric shells. Furthermore, the paper explores the optical properties of the composites at resonant frequencies and explores potential applications of systems that exhibit anomalous dispersion. The numerical observations in the paper discuss the occurrence of slow, backward, and superluminal light pulses in metal-coated dielectric and dielectric-coated metal nanocomposites with spherical Nano inclusions. Additionally, the paper suggests that incorporating gain layers with a negative dielectric function can improve the optical properties of the composite material.

**Keywords:** Anomalous dispersion, dielectric core, active dielectric core, nanocomposites, backward light



## 1. Introduction

The study of slow and superluminal light, particularly in solid-state materials at room temperature, has gained significant attention in recent years [1]. Researchers have explored various systems and composite materials to manipulate the speed of light propagation. One notable study was con- ducted by V.N. Malnev and Sisay [2], who investigated the theoretical aspects of slow, superluminal, and backward light in a composite material composed of spherical Nano inclusions embedded in active or passive host matrices. The inclusion of these nanoparticles in the composite material allowed for the control and manipulation of light propagation characteristics, such as slowing down or even reversing the direction of light. Another study [3] focused on the examination of slow and stopped light in a composite material containing spherical metallic Nano inclusions. Metallic nanoparticles can exhibit unique optical properties due to plasmonic effects, which can be utilized to control the propagation of light. By incorporating metallic Nano inclusions in the composite, the researchers were able to achieve the desired effects of slowing down and stopping light.

Systems exhibiting anomalous dispersion, particularly at resonant frequencies, can display fascinating optical properties. Anomalous dispersion refers to the situation where the refractive index of a material decreases as the frequency of light increases, contrary to the usual behavior observed in normal dispersion. The optical properties of systems with anomalous dispersion have been widely studied and reviewed [4].

*Preprint submitted to IJPR September 5, 2024*

These investigations have shed light on the fundamental aspects of light- matter interactions in these materials and their potential applications. In the context of specific experimental observations, [5] reports the measurement of the speed of superluminal light pulses in a gaseous gain-assisted atomic cesium medium. By exploiting the gain properties of the medium, researchers were able to observe and measure the superluminal propagation of light pulses. Further- more, slow light pulses have been observed in ultra-cold sodium vapor, as described in [6]. Ultra-cold atomic systems, achieved through techniques such as laser cooling and trapping, can exhibit unique optical properties due to the manipulation of atomic energy levels and interactions. These experiments demonstrated the ability to significantly slow down the propagation of light pulses through the sodium vapor.

The optical properties of metal-dielectric composites at resonant frequencies, particularly those close to the plasma frequency of the metal cover, exhibit anomalous dispersion and high levels of losses. Even at small volume fractions of the inclusions, these composites demonstrate strong anomalous dispersion. However, it is possible to significantly reduce the losses in these composites by incorporating gain elements into the host matrix or by utilizing alternating layers of composite and a gaining

medium [7, 8]. The introduction of active elements in composites can be mathematically described by incorporating a negative component in the dielectric function of the host matrix [9]. Essentially, by introducing gain elements or layers with negative dielectric function, the composite system can compensate for the losses and exhibit improved optical properties. This approach allows for enhanced control over the dispersion and losses in metal-dielectric composites, enabling the development of novel materials with tailored optical characteristics.

This paper presents the computational results obtained from the study of the refractive index and group velocity in a metal coated dielectric nanocomposites (*NCs*) with spherical Nano inclusions embedded in a linear dielectric host matrix. We show that *NCs* of spherical Nano inclusions with passive and active dielectric cores embedded in a host matrix strongly absorb light at two resonant frequencies, unlike *NCs* of dielectric coated metal spherical Nano inclusions having only one resonant frequency. The research explores both passive and active dielectric cores within the *NCs*. A small negative imaginary part in the dielectric function of the core substantially amplifies the imaginary part of refractive index and the gains. This facilitates the transmission of strongly attenuated narrow pulses of slow, backward and fast light within the *NCs* media. The author asserts that this investigation is the first to examine the occurrence of slow, backward, and fast light in *NCs* featuring spherical Nano inclusions, particularly those with metal-coated dielectric cores and dielectric-coated metal cores. The findings are deemed as original contributions to the field.

## 2. Theoretical bases and mathematical computations

Our work focused on a type of nanocomposite material called spherical metal coated dielectric nanocomposites (*NCs*). These *NCs* consist of a core made of a dielectric material with a radius of $r_1$ and a dielectric function represented by $\varepsilon_d$. The shell surrounding the core has a radius of $r_2$ and its dielectric function varies depending on the electric field applied to it, which we denote as $\varepsilon_m$. The entire nanocomposite is embedded within a host matrix made of a dielectric material with a dielectric function of $\varepsilon_h$. The nanocomposite is then exposed to incident electromagnetic radiation.

In order to investigate the impact on the refractive index and group velocity, we explored two possibilities for the dielectric function of the core. We classified the dielectric function, referred to as $\varepsilon_d$, into two categories: passive and active. The categorization depends on how the material responds to the applied electric field. This dielectric function can be written as [10, 11, 12, 13]:

$$\varepsilon_d = \varepsilon_d^{'} + i\varepsilon_d^{"} \tag{1}$$

The real and imaginary parts of the dielectric function of the core material are denoted as $\varepsilon_d'$ and $\varepsilon_d''$ respectively. When $\varepsilon_d''$ is equal to zero, the dielectric function of the core is considered passive. On the other hand, when $\varepsilon_d''$ less than zero, the dielectric function of the core is considered active. In this study, we separately examined both components of the dielectric functions to analyze their individual effects.

### 2.1. Electric potential distribution in spherical metal NCs

By applying boundary conditions and solving the Laplace's equations for spherical metal-coated dielectric *NCs*, the electric potential distributions in the core, shell, and host matrix were obtained. Consider the core-shell nanocomposite the dielectric core has a radius $r_1$ and dielectric function $\varepsilon_d$. The shell is characterized by the radius $r_2$ and dielectric function $\varepsilon_m$ (where $r_1 < r_2$). The host material is characterized by its dielectric function, denoted as $\varepsilon_h$. The electric potential distribution within the dielectric core, metallic shell, and host matrix can be described by three separate functions: ($\varepsilon_d$) for the dielectric core, ($\varepsilon_m$) for the metallic shell, and ($\varepsilon_h$) for the host matrix. These functions are derived according to the equation provided in reference [14].

$$\phi_d = -E_h A r\cos\theta, \qquad r \le r_1$$

$$\phi_m = -E_h\left(Br - \frac{C}{r^2}\right)\cos\theta, \qquad r_1 \le r \le r_2$$

$$\phi_h = -E_h\left(r - \frac{D}{r^2}\right)\cos\theta, \qquad r > r_2$$

In this case, $E_h$ represents the electric field that is applied, while r and $\theta$ represent the spherical coordinates of the point where observations are made. The z-axis is aligned with the direction of the vector $E_h$. The coefficients *A*, *B*, *C*, and *D*, are unspecified values that need to be determined using the continuity equations for the electric potential and displacement vector at the boundaries between the core-shell and shell-host matrix interfaces. At the boundary between the dielectric core and the metallic shell of a metal-dielectric nanocomposite, the electric potential is continuous. This principle stems from the fact that there cannot be a sudden jump in electric potential across the interface; therefore, the potential values in the dielectric (core) and metallic (shell) regions must be equal at the interface. This condition can be expressed as:

$$\phi_d = \phi_m \qquad r = r_1 \tag{2}$$

$$\phi_m = \phi_h \qquad r = r_2 \tag{3}$$

The continuity of the displacement vector (which is related to the electric field) must also be maintained at the interface. This condition can be expressed a

$$\varepsilon_d \frac{\partial\phi_d}{\partial r} = \varepsilon_m \frac{\partial\phi_m}{\partial r}, \qquad r = r_1 \tag{4}$$

$$\varepsilon_m \frac{\partial\phi_m}{\partial r} = \varepsilon_d \frac{\partial\phi_d}{\partial r} \qquad r = r_2 \tag{5}$$

where, the dielectric constants of the dielectric core, metal shell, and dielectric host are denoted as $\varepsilon_d$, $\varepsilon_m$, and $\varepsilon_h$, respectively. By solving equations 2, 3, 4, and 5 simultaneously, we can determine the values of the unknown Coefficients listed below:

$$A = \frac{9\varepsilon_h\varepsilon_m}{2p\nabla} \tag{6}$$

$$B = \frac{3\varepsilon_h(\varepsilon_d + \varepsilon_m)}{2p\nabla} \quad (7)$$

$$C = \frac{3\varepsilon_h(\varepsilon_d - \varepsilon_m)}{2p\nabla} r_1^3 \quad (8)$$

$$D = \left(1 - 3\varepsilon_h \frac{\varepsilon_m(3-p) + 9\varepsilon_d p}{2p\nabla}\right) r_2^3 \quad (9)$$

Where, $p = 1 - \left(\frac{r_1}{r_2}\right)^3$ is the metal volume fraction in the inclusion,

$$\nabla = \varepsilon_m^{\,2} + q\varepsilon_m + \varepsilon_d\varepsilon_h \quad (10)$$

$$q = \left(\frac{3}{2p} - 1\right)\varepsilon_d + \left(\frac{3}{p} - 1\right)\varepsilon_d \quad (11)$$

The Drude-Sommerfeld model is a theoretical framework used to describe the behavior of electrons in a metal and provides a simplified yet effective way to understand the electrical and optical properties of metals. This model provides a simple expression for the dielectric function of the metal ($\varepsilon_m$). The dielectric function represents the response of the material to an external electric field and determines its optical properties. From the Drude-Sommerfeld model, the dielectric function of the metal ($\varepsilon_m$) is given by [10, 11]:

$$\varepsilon_m = \varepsilon_\infty - \frac{1}{z(z+iz)} \quad (12)$$

Where, $\varepsilon_\infty$ represents the impact of bound electrons on polarizability. Here, $z$ is the ratio of incident radiation frequency ($\omega$) to bulk plasma frequency ($\omega_p$), and $\gamma$ is the ratio of electron damping constant ($v$) to plasma frequency ($\omega_p$). Moreover, the real and imaginary parts of $\varepsilon_m$ can be rewritten as

$$\varepsilon_m = \varepsilon'_m + i\varepsilon''_m \quad (13)$$

Where,

$$\varepsilon'_m = \varepsilon'_\infty - \frac{1}{z^2+\gamma^2} \qquad \varepsilon''_m = \varepsilon''_\infty + \frac{\gamma}{z(z^2+\gamma^2)}$$

## 3. Dispersion properties of metal-dielectric composites with spherical Nano inclusions

Dispersion refers to the phenomenon where the refractive index or other optical properties of a material vary with the frequency or wavelength of light. In the context of composites with spherical Nano inclusions, dispersion arises due to the interaction between the Nano inclusions and the surrounding matrix material. The presence of spherical Nano inclusions within a *NCs* introduces additional interfaces and interfaces, resulting in complex interactions with incident electromagnetic waves. These interactions can lead to dispersion phenomena such as frequency-dependent refractive index, absorption, and scattering.

The polarization of an individual metal covered spherical non-inclusion with a dielectric core embedded in a dielectric host matrix can be presented as follows [2, 15, 16]:

$$D = \alpha r_2^2, \qquad \alpha = 1 - \frac{3}{2}\frac{\sigma}{\nabla} \quad (14)$$

Where

$$\sigma = \varepsilon_h\left(\left(\frac{3}{2p} - 1\right) + \varepsilon_m + \varepsilon_d\right)$$

Here $D$ is the effective polarizability of the inclusion, $p = 1 - (r_1/r_2)^3$ is a metal fraction of the inclusion ($r_1$; $r_2$ are radii of the dielectric core and the metal cover, respectively). The DF of the core $\varepsilon_d$ does not depend on frequency and in general has a negative imaginary part. Since $\varepsilon_m$ and $\varepsilon_d$ are complex, the terms such as $q, \sigma, \Delta$, and $\alpha$ are also complex:

$$\Delta = \Delta' + i\Delta'', \qquad \sigma = \sigma' + i\sigma''$$

$$\alpha = \alpha' + i\alpha'' \qquad q = q' + iq''$$

Where

$$\nabla' = \varepsilon_m^{\,'2} - \varepsilon_m^{\,''2} + q'\varepsilon'_m - q''\varepsilon''_m + \varepsilon'_d\varepsilon_h$$

$$\nabla'' = 2\varepsilon'_m\varepsilon''_m + q'\varepsilon''_m + q''\varepsilon'_m + \varepsilon''_d\varepsilon_h$$

$$\sigma' = \varepsilon_h\left(\left(\frac{3}{2p} - 1\right)\varepsilon'_m + \varepsilon'_d\right)$$

$$\sigma'' = \varepsilon_h\left(\left(\frac{3}{2p} - 1\right)\varepsilon''_m + \varepsilon''_d\right)$$

$$\sigma' = 1 - \frac{3}{2}\frac{\sigma'\nabla' + \sigma''\nabla''}{\nabla'^2 + \nabla''^2}$$

$$\sigma'' = \frac{3}{2}\frac{\sigma'\nabla'' - \sigma''\nabla'}{\nabla'^2 + \nabla''^2}$$

$$q' = \left(\frac{3}{2p} - 1\right)\varepsilon'_d + \left(\frac{3}{p} - 1\right)\varepsilon'_d$$

$$q'' = \left(\frac{3}{2p} - 1\right)\varepsilon''_d$$

## 4. Refractive index of composite with passive host matrix

The effective *DF* of the composite can be obtained with the help of the Clausius Mossoti formula [16]

$$\frac{\varepsilon - \varepsilon_h}{\varepsilon + 2\varepsilon_h} = \frac{4\pi}{3} DN \quad (15)$$

Where, $D$ is given by Eq. (14) and $N$ is a density number of the inclusions. The refractive index of the composite $n$ is given by the equation

$$n^2 = \varepsilon_h\left(1 + 3f\frac{\alpha}{1 - f\alpha}\right) \quad (16)$$

where, $f = 4\pi/3r^3N$ is the volume fraction of spherical inclusions and $\alpha$ is the polarizabilityof the inclusions.

**Table 1.** Numeric values associated with physical quantities [10, 11]

| Constants | Values |
|---|---|
| $\varepsilon_d'$ | 6.0 |
| $\varepsilon_h$ | 2.25 |
| $\varepsilon_\infty$ | 4.5 |
| $\omega_p$ | $1.6 \times 10^{16}$ |
| $\nu$ | $1.68 \times 10^{14}$ |
| $\gamma$ | $1.15 \times 10^{-2}$ |

$$n^2 = \varepsilon_h \left( 1 + 3f \frac{\alpha' + i\alpha''}{1 - f\alpha' - i\alpha''} \right)$$

$$n^2 = \varepsilon_h \left( 1 + 3f \frac{\alpha' - f|\alpha|^2 + i\alpha''}{(1 - f\alpha') + (f\alpha'')^2} \right) = b_1 + ib_2 \quad (17)$$

Where,

$$b_1 = \varepsilon_h \left( 1 + 3f \frac{\alpha' - f|\alpha|^2}{\Delta f} \right)$$

$$b_2 = \left( \frac{3f\varepsilon_h \alpha''}{\Delta f} \right)$$

$$\Delta f = (1 - f\alpha')^2 + (f\alpha'')^2$$

Equating the real and the imaginary parts $n = n' + in''$ with Eq. (17) can give us the expressions

$$n'^2 - n''^2 = b_1 \quad (18)$$

$$2n'n'' = b_2 \quad (19)$$

In this representation, the real part of the refractive index is given by $n'$ and the imaginary part is given by $n''$. By separating the real and imaginary components, we can effectively express the refractive index in terms of $b_1$ and $b_2$.

$$n'^2 = \frac{1}{2}\left( \sqrt{b_1^2 + b_2^2} + b_1 \right) \quad (20)$$

$$n''^2 = \frac{1}{2}\left( \sqrt{b_1^2 + b_2^2} - b_1 \right) \quad (21)$$

These equations are used to numerically calculate the $n'$ and $n''$ of composites with metal-coated dielectric inclusions, both for passive ($\varepsilon_d'' = 0$) and active ($\varepsilon_d'' < 0$) dielectric cores. The dielectric function numerical values for the composite discussed in this section are sourced from references, with table 1 presenting the consistent values employed in numerical computations.

### 4.1. Effect of metal fractions on refractive index of metal coated dielectric spherical NCs

In figure 1(a), $n'$ versus z is depicted, while in figure 1(b), $n''$ versus z is shown, focusing on resonant frequencies of a composite material consisting of metal-coated dielectric spherical inclusions within a passive dielectric core, with varying metal fractions represented by $p$. The results illustrate two peak values of both $n'$ and $n''$ occurring at distinct resonant frequencies. Interestingly, the peak on the left side of the graph is of greater magnitude compared to the peak on the right side, evident in both $n'$ and $n''$. This discrepancy suggests an asymmetry in the behavior of the composite material concerning its refractive index properties. The substantial positive values observed in the imaginary part of the refractive index ($n''$) indicate significant absorption of electromagnetic waves at the two resonant frequencies. This absorption phenomenon implies that the composite material strongly interacts with and absorbs electromagnetic radiation at these specific frequencies as it propagates through the material.

Our results clearly demonstrate that altering the metal fraction by the same amount produces distinct $n''$ peak patterns in the passive and active dielectric core, as illustrated in figures 1(b) and 2(b). Moreover, it is noteworthy that when the metal fraction increases, the $n''$ also increases in both the passive and active dielectric core. In passive composites, as the metal fraction increases from 0.4 to 0.9, $n''$ rises from $1.9 \times 10^{-4}$ to $4.8 \times 10^{-4}$ on the left side peak and from $1.8 \times 10^{-5}$ to $7 \times 10^{-5}$ on the right side peak. Similarly, in active composites, with the metal fraction increasing from 0.4 to 0.9, $n''$ climbs from $2.7 \times 10^{-4}$ to $5.8 \times 10^{-4}$ on the left side peak and from $2 \times 10^{-5}$ to $1.1 \times 10^{-4}$ on the right side peak. The notably large positive values of the imaginary part $n''$ of the refractive index suggest strong absorption of electromagnetic waves propagating through the composite at the two resonant frequencies. Further comparison of the result from 1(b) and figure 2(b) show that the value of $n''$ occurs for each value of metal fraction (p) is larger in active dielectric core. When the radius of the core decreases, i.e., when the metal fraction (p) increases, the $n''$ of spherical metal-dielectric $NCs$ increases.

Figures 3(a) and 3(b) depict the behavior of the real part of the refractive index ($n'$) and the imaginary part of the refractive index ($n''$) respectively, for a composite material consisting of dielectric-coated metal spherical inclusions in a passive dielectric shell.

In contrast to the metal-coated dielectric spherical inclusion case, these figures show that there is only one peak value observed for both $n'$ and $n''$ in the composite with dielectric-coated metal spherical inclusions. The presence of a single peak suggests that the composite material interacts with the incident electromagnetic radiation at a specific resonant frequency.

By varying the metal fraction ($p$) of inclusions in the composite, the magnitude of the peak value changes. This variation indicates that the concentration of metal inclusions affects the optical properties of the composite material, resulting in different refractive index values. Furthermore, it is noted that in the composite with dielectric-coated metal spherical inclusions in the passive dielectric core, there is strong absorption of an incident electromagnetic wave specifically in the region of anomalous dispersion. Anomalous dispersion refers to a phenomenon where the refractive index decreases with increasing frequency. The strong absorption at this region implies that the composite material exhibits enhanced interaction and absorption of electromagnetic energy at frequencies corresponding to the anomalous dispersion regime.

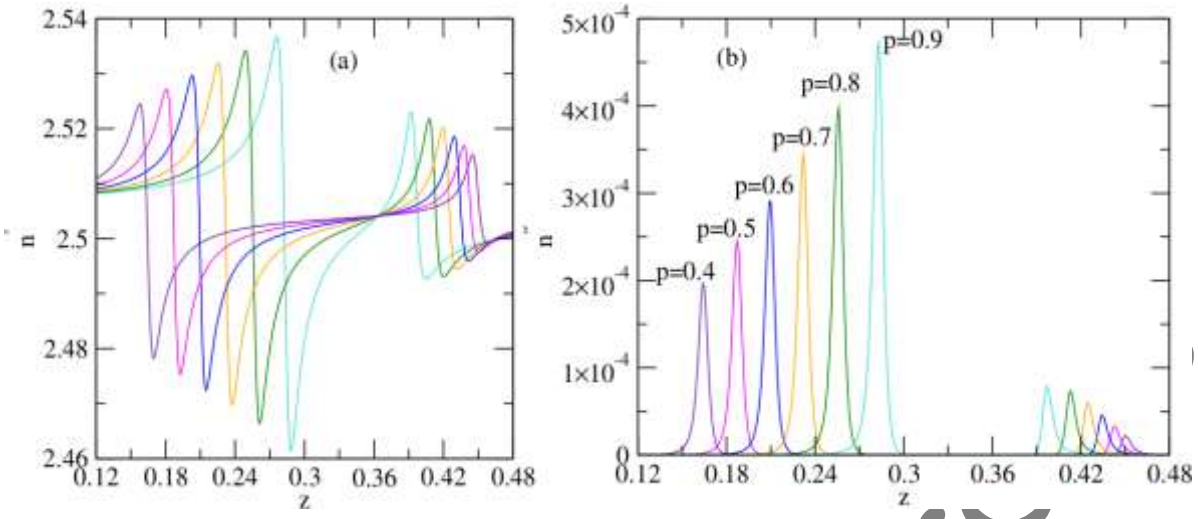


**Figure 1.** Passive composite with metal coated dielectric spherical Nano inclusions ($\varepsilon_d{}'' = 0.0$).Real part of therefractive index ($n'$) versus the dimensionless frequency ($z$) (a); imaginary part of the refractive index ($n''$) versus z (b). Numerical values of composite parameters; fraction of inclusions in the composite f = 0.001

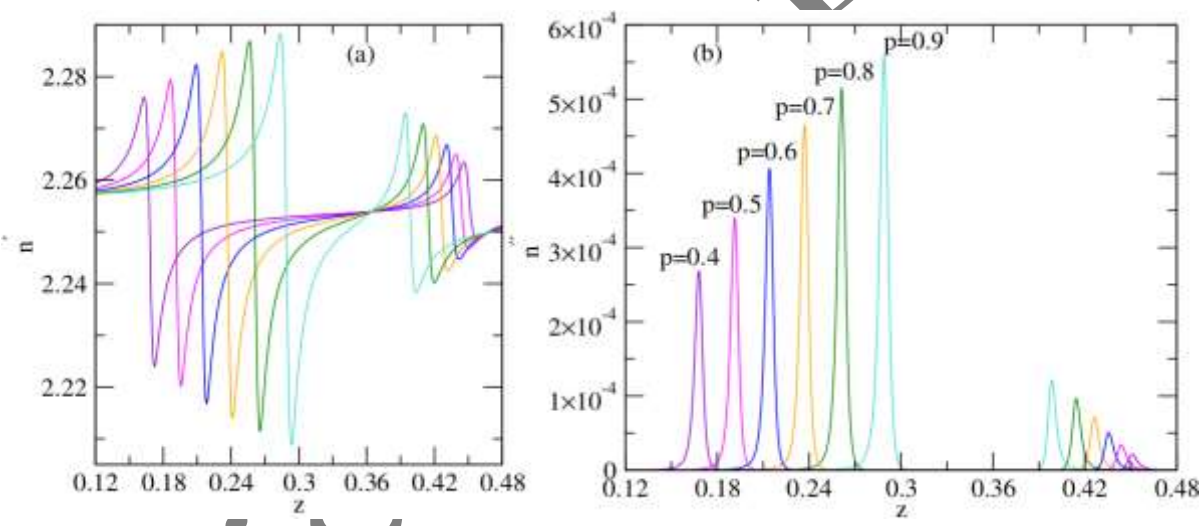


**Figure 2.** Active composite with metal coated dielectric spherical Nano inclusions ($\varepsilon_d{}'' = -0.20722$). Real part of the refractive index ($n'$) versus the dimensionless frequency ($z$) (a); imaginary part of the refractive index ($n''$) versus z (b). Numerical values of composite parameters; fraction of inclusions in the composite f = 0.001.

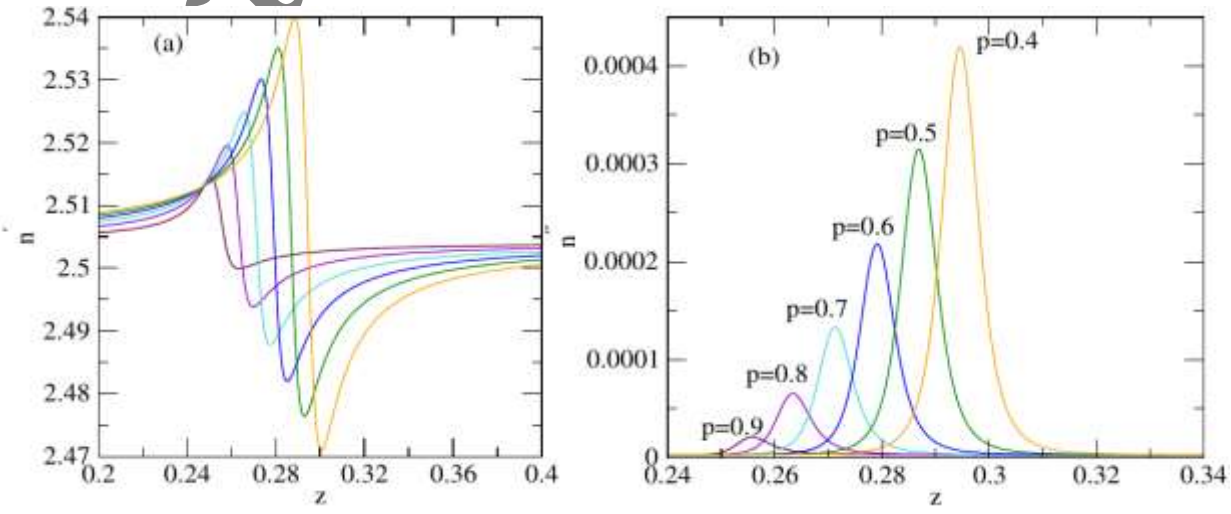


**Figure 3.** Passive composite with dielectric coated metal spherical $NCs$ ($\varepsilon_d{}'' = 0.0$). $n'$versus z (a); $n''$versus z (b). Numerical

values of composite parameters; metal fraction in the inclusion p = 0.4, 0.6, 0.7, 0.8, and 0.9, fraction of inclusions in the composite f = 0.001.

### 4.2. Effect of volume fraction of inclusion on refractive index

Figures 4a and 4b represent the behavior of the real part of the refractive index ($n'$) and the imaginary part of the refractive index ($n''$) respectively, for a composite material consisting of dielectric- coated metal spherical inclusions in a passive dielectric core. By varying the fraction of inclusions ($f$) in the composite, the magnitude of the peak value changes. This suggests that the concentration or volume fraction of the dielectric-coated metal inclusions affects the optical properties of the composite material, resulting in different refractive index values. As the volume fraction of inclusions increases, the real part of the refractive index tends to increase as well. This is because the inclusions contribute to the overall refractive index of the composite material. If the refractive index of the inclusions differs from that of the surrounding medium, the real part of the refractive index will be affected accordingly. The refractive index is an average of the refractive indices of the composite constituents, weighted by their respective volume fractions. The volume fraction of inclusions can also impact the imaginary part of the refractive index. Generally, an increase in the volume fraction of inclusions leads to an increase in the magnitude of the imaginary part of the refractive index at specific resonate frequency ($z$). This suggests that the absorption of incident electromagnetic waves by the composite material becomes stronger as the volume fraction of inclusions increases.

In dielectric-coated metal spherical nanocomposites, the refractive index is influenced by the properties of both the dielectric material and the metal core. The real part of the refractive index represents the phase velocity of light in the material, while the imaginary part corresponds to the absorption or loss of light. Figure 6, shows that when the imaginary part of the refractive index increases, it indicates an increase in the absorption or loss of light by the material. The refractive index is a complex quantity that has both a real part (related to the phase velocity of light) and an imaginary part (related to the absorption of light). In general, an increase in the imaginary part of the refractive index implies that the material is becoming more absorbing or opaque to light at a given wavelength. This increased absorption can occur due to various mechanisms, such as electronic transitions, scattering, or interactions with impurities or defects in the material. The interaction between the metal core and the dielectric coating leads to the formation of plasmons, which are collective oscillations of the conduction electrons in the metal. These plasmons can strongly interact with light, resulting in localized surface plasmon resonances (LSPRs). LSPRs are associated with peaks in the absorption spectrum and can be influenced by the refractive index of the surrounding medium.

When the imaginary component of the dielectric core is negatively enhanced, the absorption of light by the dielectric material becomes more pronounced. This heightened absorption facilitates a more efficient coupling with the plasmonic resonances in the metal core, leading to a stronger interaction between the Plasmon's and the incident light.

As a result, both the real and imaginary components of the refractive index experience an increase in their peak values. The increase in the peaks of the real part of the refractive index can be attributed to the increased interaction between the incident light and the plasmonic resonances, leading to a stronger refractive response. The increase in the peaks of the imaginary part of the refractive index is associated with the enhanced absorption and loss of light by the nanocomposite structure.

## 5. Slow, fast and backwards light

The concept of group velocity is associated with a wave packet, which is a pulse-like waveform. It refers to the velocity at which the overall shape of the wave's amplitude, known as the modulation or envelope, propagates through space [17].

$$U(x,t)=e^{i(k_x-\omega_0 t)}\int_{k_0\delta k}^{k\delta k}A(k)e^{i(kx-\frac{d\omega}{dx}|k_0 t)(k-k_0)} \quad (22)$$

Equation (22) represents the wave packet, where $U(x, t)$ is the function describing the pulse. It shows that the pulse maintains its shape without distortion as it travels, and it has a specific velocity called the group velocity ($V_g$), as given by equation (23).

$$\upsilon_g=\frac{d}{dk}|k_0 \quad (23)$$

The group velocity can also be expressed in terms of the group refractive index, which characterizes how light propagates in a medium.

$$\upsilon_g=\frac{c}{n'(\omega)+\omega\frac{dn'(\omega)}{d\omega}}=\frac{c}{n_g}, \quad (24)$$

where $c$ is the speed of light in vacuum and $n_g$ is the group index. This expression allows us to discuss the concepts of slow, fast, and negative group velocities of light by considering the behavior of the group refractive index.

To determine the numerical values of the group velocity near and at the resonant frequency, we can make use of equation (20), where the real part of the refractive index is described as a function of the dimensionless frequency z. The parameters utilized for calculating the group velocity remain consistentwith those used for determining the real and imaginary parts of the refractive index. The equation for the group velocity is as follows:

$$\upsilon_g=\frac{c}{n'(z)+z\frac{dn'(z)}{dz}}=\frac{c}{n_g}, \quad (25)$$

In this equation, the group velocity ($v_g$) is obtained by dividing the speed of light in a vacuum (c) by the sum of the first derivative of the refractive index with respect to z ($n'(z)$) and the product of z and the derivative of the refractive index with respect to z ($zdn'(z)/dz$). Alternatively, the group velocity can be expressed as the

ratio of the speed of light in a vacuum to the group index ($n_g$).

The second term in the equation ($z\frac{n'(z)}{\mathrm{d}(z)}$ ) plays a crucial role in determining the extreme values of the group velocity. When the group velocity (vg) is much smaller than the speed of light in Vacuum (c), it is known as "slow light"($v_g > c$). In the case of normal dispersion, where $\frac{n'(z)}{dz} > 0$. And $n > 1$, the group velocity is lower than the phase velocity. Conversely, "fast light" refers to light that travels faster than the speed of light in a vacuum, which occurs when $v_g > c$. Slow and fast light refer to the speed of the group velocity relative to the speed of light in a vacuum. Additionally, "slow backward light" describes light that moves slower than the speed of light in a vacuum, which can happen when $v_g > -c$ or when the group velocity is small and negative. On the other hand, "fast backward light" corresponds to light that travels faster than the speed of light in a vacuum, which occurs when $v_g > -c$ or when the group velocity is large and negative. Slow backward and fast backward light refer to the direction of the group velocity relative to the phase velocity. In regions of anomalous dispersion, $\frac{n'(z)}{dz}$ can become significantly negative. Consequently, the group velocity can differ significantly from the phase velocity, often exceeding $c$ or even becoming negative [6].

In the presented analysis, we investigate different types of light waves propagating through our composites. To evaluate these waves, we employ two measures: the group velocity index $n_g$ and the normalized group velocity $v_g(z)/c$. These measures are determined by computing the real part of the refractive index $n'(z)$ using the initial equation (20) for both passive and active dielectric core composites.

### 5.1. Effect of metal fraction on group velocity of spherical metal-dielectric NCs

The numerical results obtained for the passive dielectric core are illustrated in figure 7, representing the variations of $n_g$ and $v_g$ with respect to $z$ for a passive composite containing metal-dielectric spherical Nano inclusions with parameters $f = 0.001$ and $\varepsilon_d'' = -0.0$. In figure 7(a), it can be observed that $n_g(z)$ reaches zero at two different frequencies. The first minimum occurs around −0.8, indicating slow backward light, while the second minimum occurs around 0.4, suggesting slow light. Figure 7(b) shows that, for $p = 0.9$ in the vicinity of the second resonant frequency, the group velocity of fast light is$v_g = 3.1c$. In the region of the first resonant frequency, there are two points of singularity. As the frequency approaches the first asymptote line from the left, as well as from the right to the first asymptote line, the ratio $v_g/c$ tends to positive infinity. Between the two asymptote lines on the left side, a negative superluminal light with a group velocity of $v_g = -1.3c$ is obtained. Figures 8(a) and (b) display the variations of $n_g$ and $v_g$ with respect to $z$ for the active compos it containing metal-dielectric Nano inclusions with $f = 0.001$ and $\varepsilon_d''$=−0.20722. In figure 8(a), it can be observed that $n_g(z)$ equals zero at four different frequencies. The first minimum occurs at approximately -2.3, while the second minimum is around 0.6.

Figure 8 illustrates the behavior of the active dielectric core. In this particular outcome, there are five distinct branches of $v_g/c$. Among these branches, three exhibit positive values of $v_g/c$ , indicating a positive group velocity. This suggests that the speed at which the overall shape or envelope of a wave packet propagates is greater than the speed of light. Conversely, two branches display negative values of $v_g/c$, indicating a negative group velocity. A negative group velocity implies that the overall wave packet appears to propagate backward in space.

The negative group velocity observed in the active composite is typically a result of a phenomenon known as anomalous dispersion. The positive and negative group velocity branches are distinguished by two pairs of nearby asymptotes. These asymptotes, which the graph approaches but never intersects, coincide with the points where $n_g$ equals zero. When the frequency approaches these paired asymptotes from beyond, the group velocity $v_g$ heads towards positive infinity ($v_g \rightarrow +\infty$). Conversely, as the frequency nears the asymptotes from within, the group velocity trends towards negative infinity ($v_g \rightarrow -\infty$).

From the results of passive composites illustrated in figure 9(b), we can draw observations regarding group velocities across different frequencies and metal fraction values. At the appropriate resonant frequency ($f = 0.001$), the group velocities for fast light are documented as $v_g = 1.4c$, $v_g = 2.45c$, and $v_g = 2.8c$ for metal fraction values $p = 0.99$, $p = 0.96$, and $p = 0.93$ respectively. These findings suggest that the system demonstrates superluminal group velocities, exceeding the speed of light, at the specified frequencies and metal fraction values. In the vicinity of the first resonant frequency, there are two singular points present. As the frequency approaches these points from both the left and right directions, the group velocity tends towards positive infinity (+∞). In the region between the two asymptote lines on the left side, the system demonstrates negative superluminal group velocities. Specifically, for $p = 0.99$, $p = 0.96$, and $p = 0.93$, the system exhibits group velocities of $v_g = -0.5c$ (slow backward light), $v_g = -0.72c$ (slow backward light), and $v_g = -1.1c$ (fast backward light), respectively.

When the thickness of a metal inclusion is reduced, it has notable effects on the behavior of light. Specifically, the group velocity of fast light increases, while the group velocity of backward light decreases. This implies that by decreasing the thickness of the metal inclusion, the behavior of light is altered, resulting in faster propagation for certain modes (fast light) and slower propagation for others (backward light). This observation highlights the crucial role played by the thickness of the metal inclusion in determining the specific characteristics of light propagation within the studied system.

In figures 10(a) and (b), the variations of $n_g$ and $v_g$ with respect to $z$ are illustrated for the active composite consisting of metal-dielectric nanocomposites (*NCs*) with a metal fraction of $f = 0.001$ and a negative imaginary part of the dielectric constant of the active dielectric core, $\varepsilon_d'' = -0.20722$.

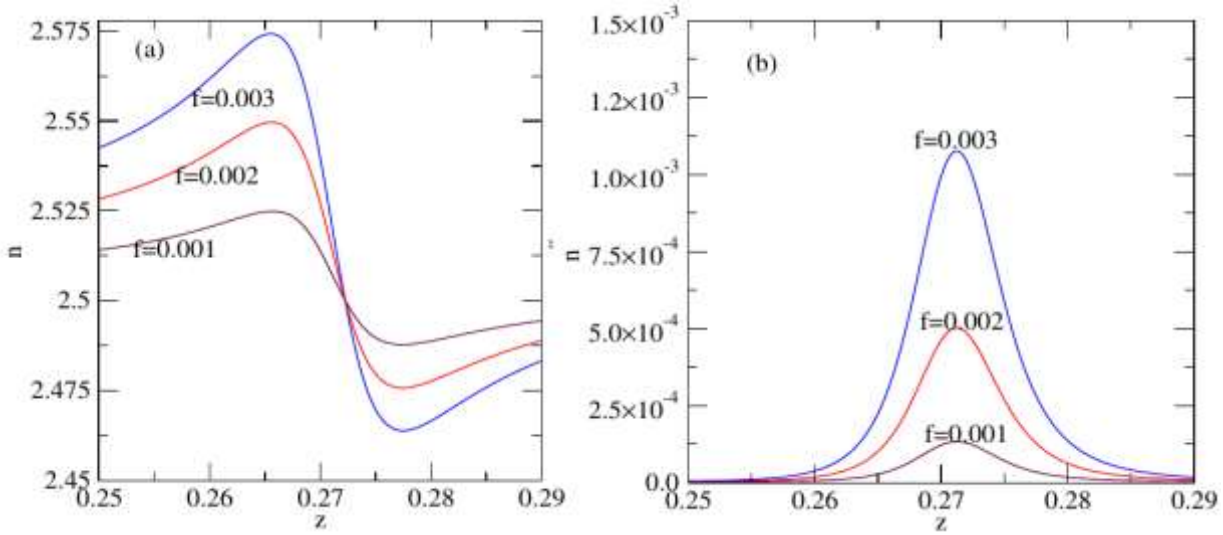


**Figure 4.** Passive composite with dielectric coated metal spherical *NCs* ($\varepsilon_d{}''= 0.0$). $n'$ versus z (a); $n''$ versus z (b). Numerical values of composite parameters; metal fraction in the inclusion p = 0.7.

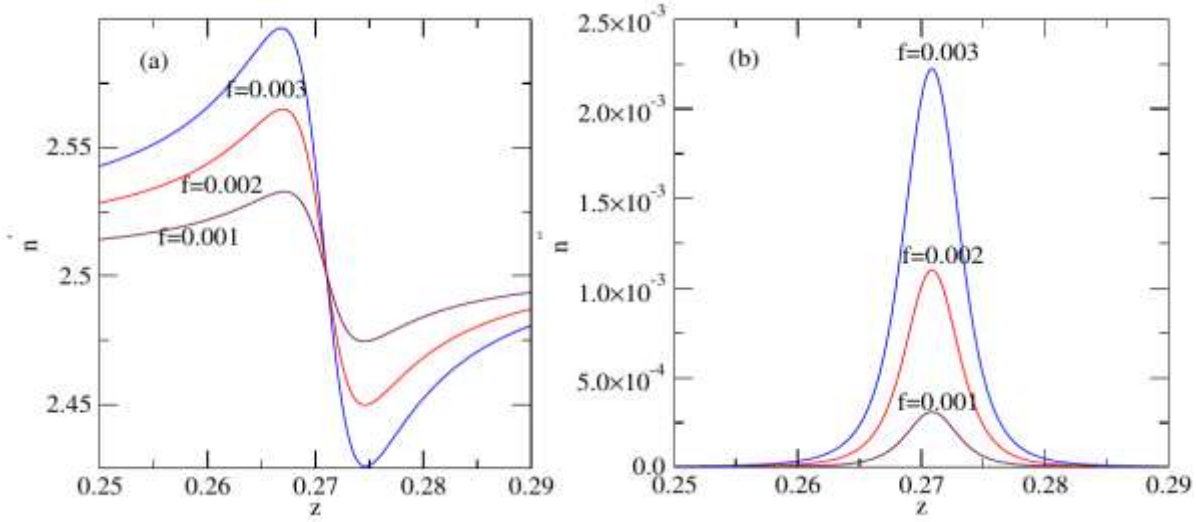


**Figure 5.** Active composite with dielectric coated metal spherical NCs ($\varepsilon_d{}''= -0.20722$). $n'$ versus z (a); $n''$ versus z (b). Numerical values of composite parameters; metal fraction in the inclusion p = 0.7.

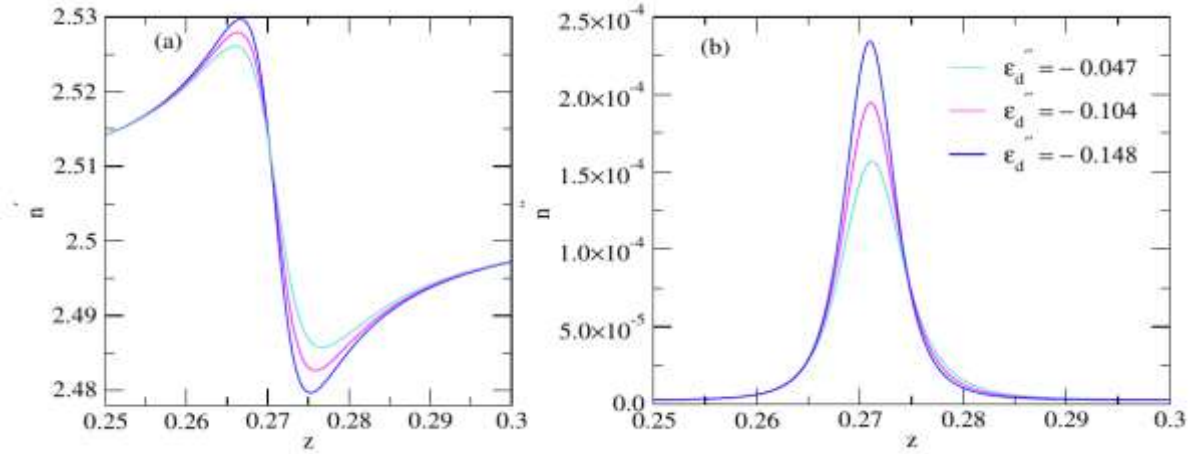


**Figure 6.** Active composite with dielectric coated metal spherical *NCs* with three different values of $\varepsilon_d{}''= 0.0$). $n'$ versus z (a); $n''$ versus z (b). Numerical values of composite parameters; metal fraction in the inclusion p = 0.7.

From these figures, it is evident that as the metal fraction of the spherical metal-dielectric $NCs$ increases, the first pair of asymptotes and the second pair of asymptotes experience blue shift and red shift, respectively. This means that the first pair of asymptotes move towards larger values of $z$ or shorter wavelengths, while the second pair of asymptotes shift towards smaller values of $z$ or longer wavelengths.

As a result, the horizontal positions between the corresponding asymptotes of $v_g/c$ become closer to each other. As the metal fraction increase in the active composite leads to a shift in the positions of the asymptotes, causing the corresponding asymptotes of $v_g/c$ to come closer together in terms of their horizontal positions.

From figure 10(b) the distance between the asymptotes affects the behavior of negative group velocities. If the distance between the asymptotes is narrower, the maxima of negative $v_g$ become "deeper," indicating more pronounced negative group velocities. Within the frequency range between the asymptotes, negative group velocities are observed, which corresponds to "negative light." This means that the wave packet appears to propagate in the reverse direction compared to the phase velocity. Outside of these asymptotes, the group velocities are normal ($v_g < c$), meaning they are positive and less than the speed of light. Additionally, superluminal (faster than light) group velocities can also be observed in this region.

According to the data presented in figure 10(b), the group velocity $v_g$ demonstrates peaks within the left and right sets of asymptotes at specific values of $p$. Within the left set of asymptotes, $v_g$ reaches maximum values of $v_g = -0.47, v_g = -0.4$, and $v_g = -0.49\ for\ p = 0.93, p = 0.96$, and $p = 0.99$, respectively. Similarly, within the right set of asymptotes, $v_g$ attains maximum values of $v_g = -1.15, v_g = -1.1$, and $vg = -1.5\ for\ p = 0.93, p = 0.96, and\ p = 0.99$, respectively. These maxima highlight the extreme values that the group velocity can attain within the active composite. They represent specific points in the frequency range where the group velocity reaches its highest negative values. The different values of $p$ correspond to different conditions or parameters of the system, and they determine the precise locations and magnitudes of these maxima. These results are in agreement with [18], where it was first shown that the superluminal and backward light can be characterized by the group velocity.

### 5.2. Effect of volume fractions on group velocity of dielectric-metal NCs

In our investigation, we analyzed the effect of inclusion volume fractions on the group velocity of spherical dielectric-coated metal nanocomposites ($NCs$) by considering both passive and active dielectric shells. We observed that as the volume fraction of inclusions increases while keeping $p$ constant, the peaks of $n_g$ decrease at specific dimensionless frequencies ($z$).

The results for waves in passive dielectric shells of $NCs$ with dielectric-coated metal inclusions are presented in figure 11, while figure 12 shows the corresponding results for waves in active dielectric shells.

In passive composites depicted in figure 11(b), $v_g/c$ showcases a single branch of positive light. This positive light can propagate within the composite media with a group velocity of $v_g = 1.27c$, marking the maximum group velocity observed in passive dielectric-coated metal composites.

In active composites, we examine those with $\varepsilon_d'' = -0.20722$ and $f = 0.001$, exhibiting a single resonant frequency. As seen in figure 12(a), $n_g$ exhibits a solitary minimum. Correspondingly, in figure 12(b), $v_g/c$ displays two branches of positive light and one branch of negative light. The negative light can propagate within the composite media with a group velocity of $v_g = -0.53c$, representing the maximum group velocity. It's noteworthy that the absorption control parameter $n''$ is highly sensitive to the value of $\varepsilon_d''$, practically demonstrating a linear dependence on $f$ when small.

Figures 13 and 14 present the numerical outcomes for the group index and group velocity of a composite material consisting of metal spherical inclusions coated with dielectric, enclosed within a passive and active dielectric shell. The results are shown for four different volume fraction of inclusions: $f = 0.0005, f = 0.001, f = 0.002$, and f = 0.003. The curves representing the ratio of group velocity to the speed of light ($v_g/c$) demonstrate that as the dimensionless frequency z approaches the first asymptote from the left and the second asymptote from the right, $v_g/c$ tends towards positive infinity. However, within the range between these two singularity points, the material exhibits characteristics of slow light, fast light, and slow backward light.

Figure 13 specifically illustrates that the group velocity of slow light, at $v_g/c = 0.65$ for f = 0.0005, transitions to fast light at $v_g/c = 1.5$ for f = 0.001. Additionally, the group velocities of backward light, at $v_g/c = -1.5$ for f = 0.002, shift to $v_g/c = -0.5$ for f = 0.003. On the other hand, in the presence of an active dielectric shell with $\varepsilon_d'' = -0.20722$, the group velocity at f = 0.0005 becomes $v_g = 3.4c$. For the remaining volume fractions of inclusions, figure 14(b) shows the presence of slow backward light. The result also show that the effect of volume fractions of inclusion on the group velocity is different in passive and active dielectric shell of the spherical dielectric coated metal $NCs$. Generally, the results agree with other research findings in that varying the volume fractions of inclusion plays an important role in determining the resonance positions of the group index and group velocity in nanocomposites [19].

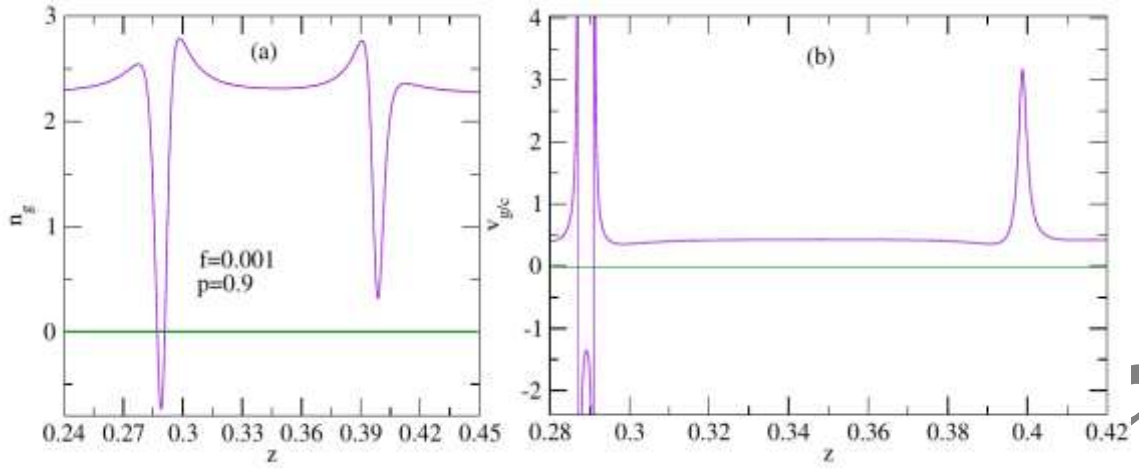


**Figure 7.** Passive composite with metal-dielectric spherical Nano inclusions ($\varepsilon_d{''}= 0$). Its group index $n_g$ versus the dimensionless frequency $z$ (a). The normalized group velocity $v_g/c$ versus $z$ (b). Numerical values of composite parameters: metal fraction in an inclusion p = 0.9, fraction of inclusions in the composite f = 0.001.

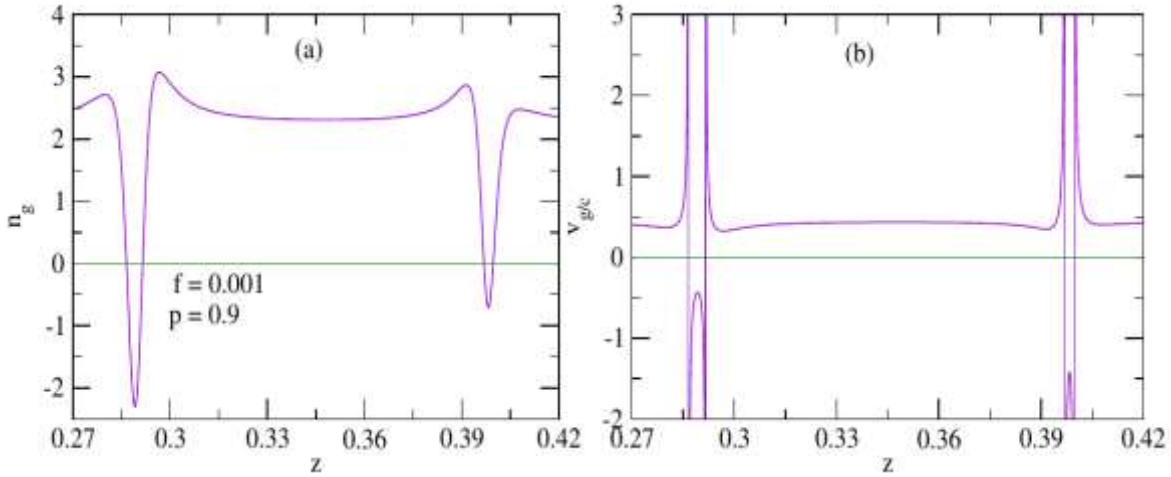


**Figure 8.** Active composite with metal-dielectric spherical Nano inclusions ($\varepsilon_d{''}= -0.20722$). Its group index $n_g$ versus the dimensionless frequency $z$ (a). The normalized group velocity $v_g/c$ versus $z$ (b). Numerical values of composite parameters: metal fraction in an inclusion p = 0.9, fraction of inclusions in the composite f = 0.00.1.

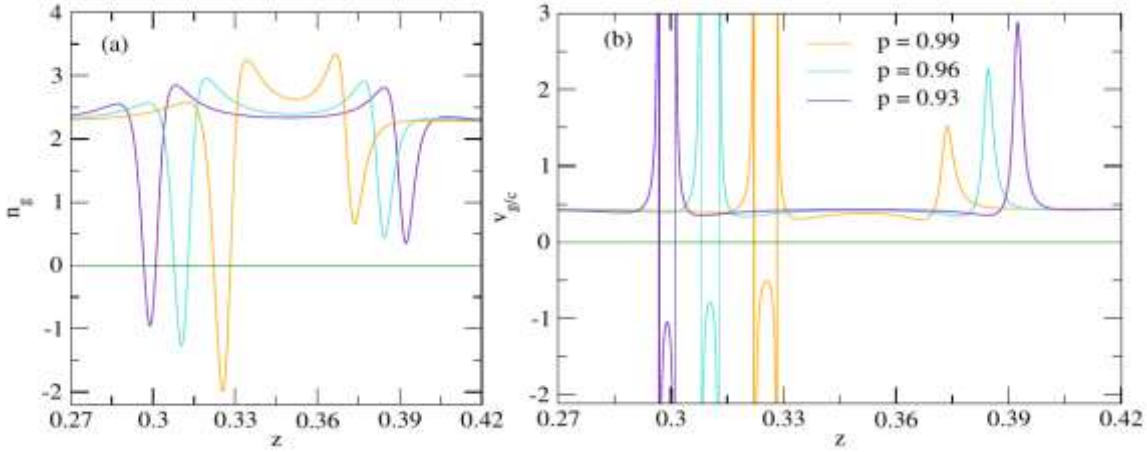


**Figure 9.** Passive composite with metal-dielectric spherical Nano inclusions ($\varepsilon_d{''}= -0.0$). Its group index $n_g$ versus $z$ (a). The normalized group velocity $v_g/c$ versus $z$ (b). Numerical values of composite parameters: three different metal fraction in an inclusion, fraction of inclusions in the composite f = 0.001.

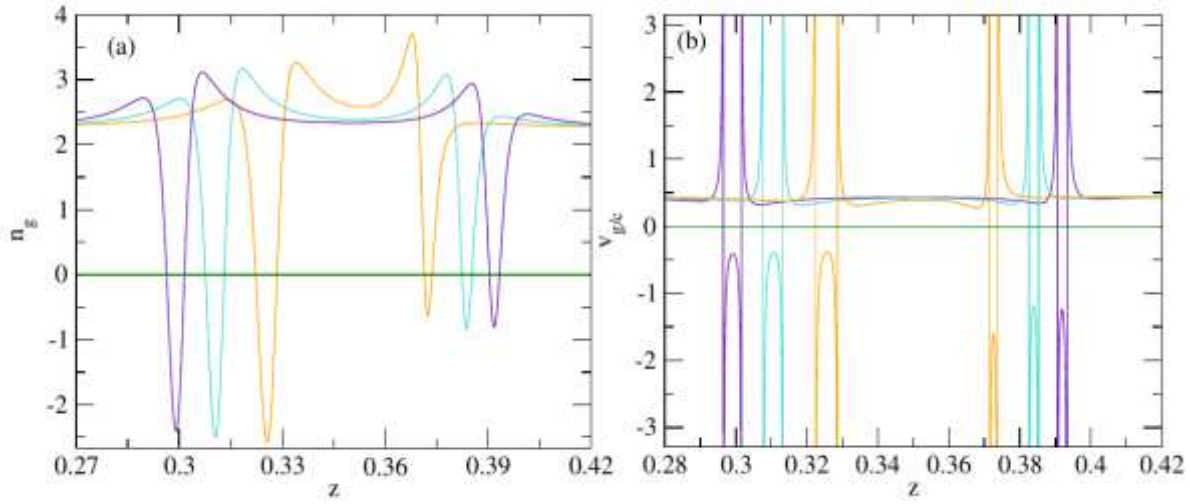


**Figure 10.** Active composite with metal-dielectric spherical Nano inclusions ($\varepsilon_d{''}$= −0.20722). Its group index $n_g$ versus $z$ (a). The normalized group velocity $v_g/c$ versus $z$ (b). Numerical values of composite parameters: three different metal fraction in an inclusion, fraction of inclusions in the composite f = 0.001.

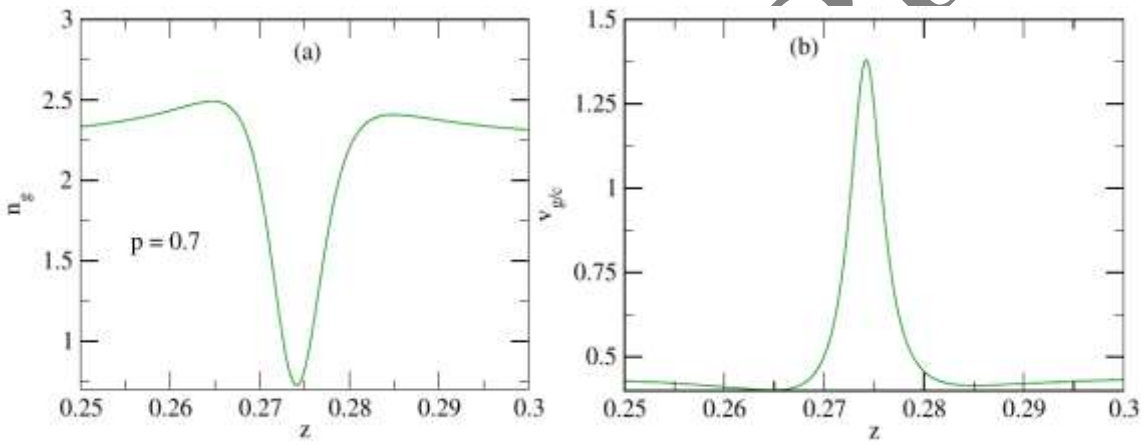


**Figure 11.** Passive composite with dielectric-metal spherical Nano inclusions ($\varepsilon_d{''}$= −0.0). Its group index $n_g$ versus $z$ (a). The normalized group velocity $v_g/c$ versus $z$ (b). Numerical values of composite parameters: metal fraction in an inclusion $p$ = 0.7.

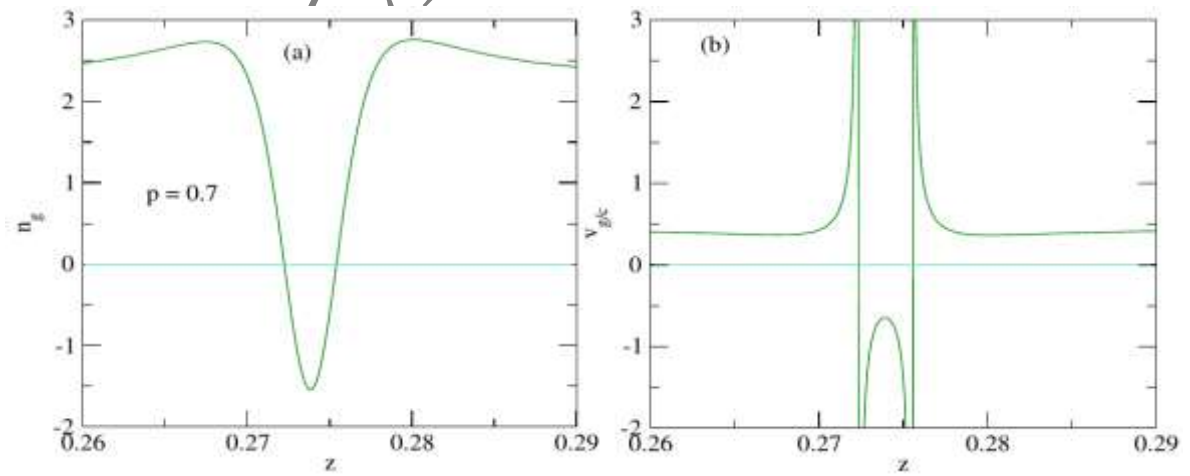


**Figure 12.** Active composite with dielectric-metal spherical Nano inclusions ($\varepsilon_d{''}$= −0.20722). Its group index $n_g$ versus $z$ (a). The normalized group velocity $v_g/c$ versus $z$ (b). Numerical values of composite parameters: metal fraction in an inclusion $p$ = 0.7.

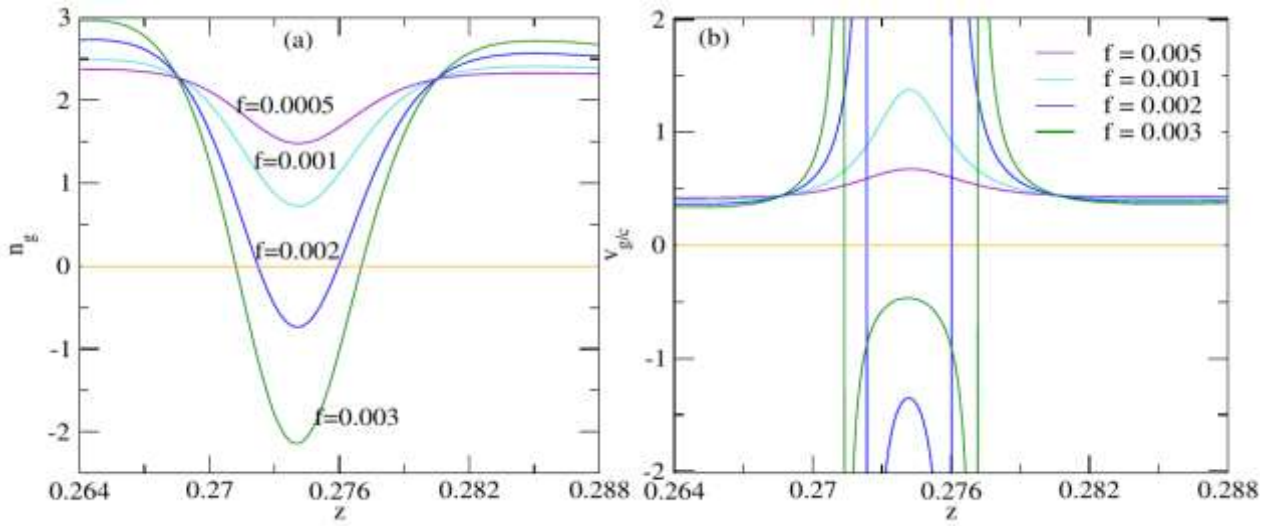


**Figure 13.** Passive composite with dielectric-metal spherical Nano inclusions ($\varepsilon_d{}'' = -0.0$). Its group index $n_g$ versus $z$ (a). The normalized group velocity $v_g/c$ versus $z$ (b). Numerical values of composite parameters: metal fraction in an inclusion $p = 0.7$

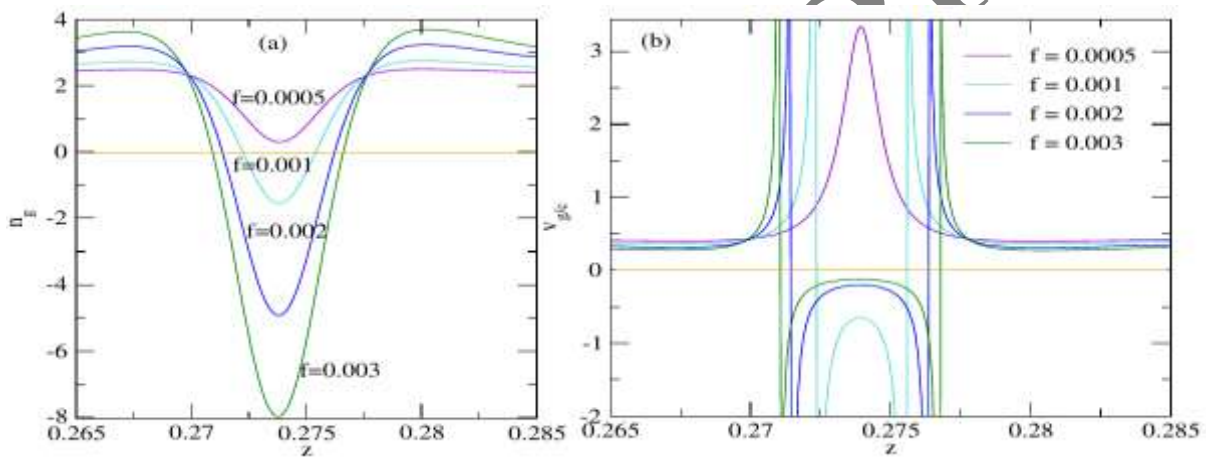


**Figure 14.** Active composite with dielectric-metal spherical Nano inclusions ($\varepsilon_d{}'' = -0.20722$). Its group index $n_g$ versus $z$ (a). The normalized group velocity $v_g/c$ versus $z$ (b). Numerical values of composite parameters: metal fraction in an inclusion $p = 0.7$

## 6. Conclusions

This research demonstrates the capacity to effectively manipulate the speed of light in composite materials. These composites consist of metal coated dielectric and dielectric coated metal spherical inclusions embedded within passive and active dielectric cores and shells. The study reveals that light pulses can travel at varying velocities within these composites, encompassing both slower and faster speeds, and even exhibiting backward propagation. One of the primary challenges in achieving long-distance propagation of light pulses within composites featuring metal coated dielectric and di- electric coated metal inclusions within a passive dielectric core is the significant absorption displayed by the composite. However, by introducing a negative component to the imaginary part of the permittivity, it becomes possible to substantially mitigate the issue of electromagnetic wave attenuation within the composite. The fraction of metal in the metal coated dielectric spherical inclusions ($p$), plays a pivotal role in controlling the speed of light or electromagnetic waves propagating through these composites. Conversely, in composites with dielectric coated metal inclusions, the fraction of inclusions ($f$), influences the outcomes related to wave speed. Considering the controllable nature of light speed in these model nanocomposites, they hold great promise for a variety of optical applications. These applications include optical communications, photonic circuitry, sensing and imaging, metamaterials, and quantum optics.

## Data Availability Statement

This manuscript has no associated data or the data will not be deposited.

## Conflicts of interest

The author has no conflicts to declare.

## References


1. M S Bigelow, N Lepeshkin, and R Boyd, *J. Phys. Condens. Matter* **16** (2004) R1321.
2. V Malnev and S Shewamare, *Phys. B: Condens. Matter* **426** (2013) 52.
3. K H Kim and S H Choe, *Ann. Phys*. **529** (2017) 1700103
4. R W Boyd, *J. Mod. Opt*. **56** (2009) 1908.
5. L J Wang, A Kuzmich, and A Dogariu, *Nature*, **406** (2000) 277.
6. L V Hau, et al., *Nature*, **397** (1999) 594.
7. A K Sarychev and G Tartakovsky, *Phys. Rev*. B **75** (2007) 085436.
8. S A Ramakrishna and J B Pendry, *Phys. Rev*. B **67** (2003) 201101.
9. A V Dorofeenko, et al., *Phys.-Uspekhi* **55** (2012) 1080.
10. Physics-Uspekhi, 55, 1080
11. S Getachew, et al., *Adv. Condens. Matter Phys*. (2024).
12. S Getachew, et al., *Int. J. Curr. Res*. (2023) 15.
13. T T Hirpha, et al., *AIP Adv*. **14** (2024) 1.
14. T T Hirpha, et al., *Mater. Res. Express* **10** (2023) 045005.
15. 045005
16. O Buryi, et al., *Ukr. J. Phys*. **56** (2011) 311.
17. 311-311
18. S Shewamare and V Malnev, *Phys.* B *Condens. Matter* **407** (2012) 4837.
19. C F Bohren and D R Huffman, "*Absorption and scattering of light by small particles*" John Wiley & Sons (2008).
20. J D Jackson and R F Fox, "*Classical electrodynamics*" (1999).
21. C Garrett and D McCumber, *Phys. Rev.* A **1** (1970) 305.
22. Y Abbo, *Ukr. J. Phys*. **66** (2021) 281.